Effects of the *FHL2* gene on the development of subcutaneous and intramuscular adipocytes in goats

An Li[1,2,3], Youli Wang[1,3], Yong Wang[1,2,3], Yan Xiong[1,2,3], Yanyan Li[1,2,3], Wei Liu[1,3], Jiangjiang Zhu[1,2] and Yaqiu Lin[1*]

Abstract

Background   Adipose tissue affects not only the meat quality of domestic animals, but also human health. Adipocyte differentiation is regulated by a series of regulatory genes and cyclins. Four and half-LIM protein (FHL2) is positively correlated with the hypertrophy of adipocytes and can cause symptoms such as obesity and diabetes.

Result   In the transcriptome sequencing analysis of intramuscular adipocytes after three days of differentiation, the differentially expressed gene *FHL2* was found. To further explore the biological significance of the differentially expressed gene *FHL2*, which was downregulated in the mature adipocytes. We revealed the function of *FHL2* in adipogenesis through the acquisition and loss of function of *FHL2*. The results showed that the overexpression of *FHL2* significantly increased the expression of adipogenic genes (*PPARγ*, *C/EBPβ*) and the differentiation of intramuscular and subcutaneous adipocytes. However, silencing *FHL2* significantly inhibited adipocyte differentiation. The overexpression of *FHL2* increased the number of adipocytes stained with crystal violet and increased the mRNA expression of proliferation marker genes such as *CCNE*, *PCNA*, *CCND* and *CDK2*. In addition, it significantly increased the rate of EdU positive cells. In terms of apoptosis, overexpression of *FHL2* significantly inhibited the expression of *P53* and *BAX* in both intramuscular and subcutaneous adipocytes, which are involved in cell apoptosis. However, overexpression of *FHL2* promoted the expression of *BCL*, but was rescued by the silencing of *FHL2*.

Conclusions   In summary, *FHL2* may be a positive regulator of intramuscular and subcutaneous adipocyte differentiation and proliferation, and acts as a negative regulator of intramuscular and subcutaneous adipocyte apoptosis. These findings provide a theoretical basis for the subsequent elucidation of FHL2 in adipocytes.

Keywords   FHL2, Goat, Adipogenesis, Subcutaneous adipocytes, Intramuscular adipocytes

---

*Correspondence:
Yaqiu Lin
linyq1999@163.com
[1]Key Laboratory of Qinghai-Tibetan Plateau Animal Genetic Resource Reservation and Utilization of Education Ministry, Southwest Minzu University, Chengdu, China
[2]Key Laboratory of Qinghai-Tibetan Plateau Animal Genetic Resource Reservation and Exploitation of Sichuan Province, Southwest Minzu University, Chengdu, China
[3]College of Animal & Veterinary Science, Southwest Minzu University, Chengdu, China

Introduction

Adipose tissue is multifunctional and affects not only the meat quality of domestic animals, but also human health [1–3]. In domestic animals, the distribution of adipose tissue affects meat taste and carcass mass [4–6]. In humans, adipose tissue is closely related to many major diseases such as diabetes and obesity [7–9]. Therefore, elucidating the development of adipose tissue and the molecular mechanisms of their regulation is essential for human life and health. Many studies have reported that the adipocyte differentiation is regulated by a series of regulatory genes, such as peroxisome proliferator activated receptor gamma (*PPARγ*), CCAT enhancer binding protein (*C/EBPα*) and cyclin D1 (*CCND*) [10, 11].

In the transcriptome sequencing analysis of intramuscular adipocytes after three days of differentiation, we focused on FHL2, which was downregulated in the mature intramuscular adipocytes. FHL2 is a member of the LIM-only subclass of the LIM protein superfamily [12], which is widely distributed in different cells (epithelial cells), forms different tissues (ovaries and muscles), and finally forms different organs [13–15]. *FHL2* has been shown to play an important role in differentiation, proliferation of skeletal muscle satellite cells and inducing apoptosis in mesangial cell [16–18]. In addition, *FHL2* is positively correlated with the hypertrophy of adipocytes and can cause symptoms such as obesity and diabetes [19, 20]. In addition, *FHL2* regulates the expression of many transcriptional genes. For example, overexpression of *FHL2* leads to downregulated expression of cylin D1 (*CCND*) and upregulated expression of *P21* and *P27*, thereby inhibiting the cell proliferation of murine fibroblasts [21]. The E4 transcription factor (*E4F1*) is associated with *FHL2* and inhibition of *E4F1*, which represses cell proliferation [22]. In osteoblasts, *FHL2* stimulates osteoblast differentiation and contributes to bone formation [23]. *FHL2* may be associated with radiation-induced apoptosis [24], as a marker gene for apoptosis, the presence of FHL2 increases P53 expression, in addition to enhancing P53 expression in turn stimulating FHL2 expression [25]. In addition, transient overexpression of SKI protein (SKI) and *FHL2* in ski (-/-) melanocytes synergistically enhanced cell growth [26]. These different studies show that *FHL2* performs different functions in nonbiological processes. It remains unclear whether *FHL2* regulates the development of the goat subcutaneous and intramuscular adipocytes.

Therefore, the function of *FHL2* in regulating the development of adipocytes was revealed by using goat intramuscular and subcutaneous adipocytes in vitro. First, the coding sequence of the goat *FHL2* gene was cloned, and its function in intramuscular and subcutaneous adipocytes was explored by silencing and overexpression techniques. Oil Red O, BODIPY and EdU staining were used to determine the effect of *FHL2* on the differentiation and proliferation of adipocytes, and MTT was used to detect the effect of *FHL2* on the cell proliferation. In addition, flow cytometry was used to detect the effect of *FHL2* on adipocyte apoptosis. Finally, real time quantitative polymerase chain reaction (RT-qPCR) was used to detect the expression of differentiation, proliferation, and apoptosis marker genes. *FHL2* may be a positive regulator of intramuscular and subcutaneous adipocyte differentiation and proliferation, and acts as a negative regulator of intramuscular and subcutaneous adipocyte apoptosis. These findings provide a theoretical basis for the subsequent elucidation of *FHL2* in adipocytes.

Results

Screening of *FHL2* gene

Filters for differentially expressed genes between preadipocytes and mature adipocytes can promote further study of fat deposition in goats. Numerous studies have shown that RNA-seq helps reveal transcriptome differences in tissues and cells [27–30]. In this study, the DEG-Seq was used to analyse the DEGs in intramuscular preadipocytes and adipocytes. When the p value < 0.05, we obtained 4749 DEGs, of which 2556 were upregulated and 2193 were downregulated (Fig. 1A). Studies have shown that *FHL2* plays an important regulatory role in the development of adipocytes. Therefore, we focused on *FHL2*, which is downregulated in mature intramuscular adipocytes and validated by RT-qPCR. The expression of *FHL2* in mature intramuscular adipocytes was lower than in intramuscular preadipocytes, which was consistent with the RNA-seq trend (Fig. 1B).

Cloning of the *FHL2* gene in goats, and its tissue and time expression profile

To further explore the biological significance of FHL2, the cDNA of goat triceps tissue was used as template, and the primers FHL2-S and FHL2-A were used. The FHL2 gene was successfully cloned after PCR amplification. The *FHL2* gene fragment was cloned with a length of 1353 bp (Fig. 2A), in which the CDS region is 838 bp with the start codon ATG and stop codon TGA, while the 5' UTR was 779 bp and the 3'UTR was 338 bp (Fig. 2B). RT-qPCR was used to detect the expression level of FHL2 gene in various goat tissues, and the results showed that FHL2 gene was expressed in 8 tissues. FHL2 expression is significantly higher in the heart and kidneys than in other tissues ($P < 0.05$, Fig. 2C). The results showed that the expression of *FHL2* gene was specific in tissues. The results
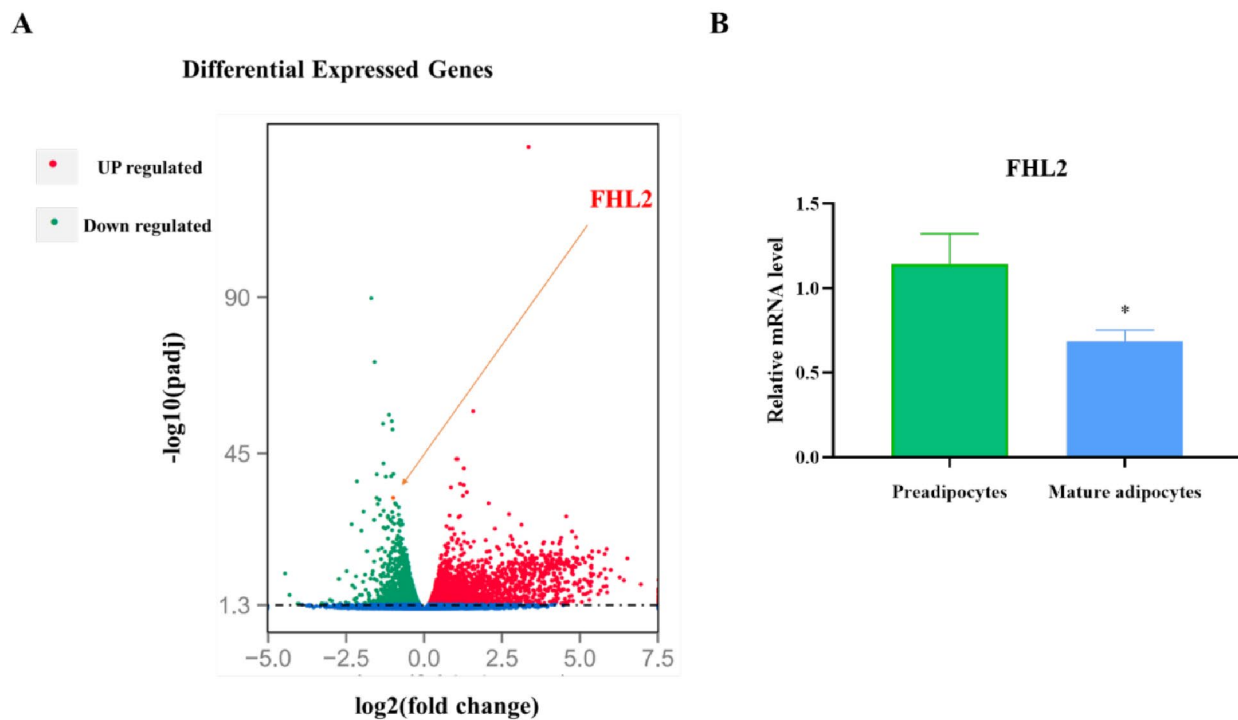
A

Differential Expressed Genes

B

Fig. 1 Transcriptome sequencing comparison of mature adipocytes and preadipocytes. **A** Volcano plot of DEGs. Volcano plot of DEGs in preadipocytes and mature adipocytes, the screening condition is $P < 0.01$; **B** Validation of DEGs by PCR. Validation of differential expression gene using RT-qPCR ($n = 5$). The RT-qPCR data were analyzed using $2^{-\Delta\Delta Ct}$ method, and ubiquitously expressed transcript (*UXT*) was used as endogenous control. "*" denotes $P < 0.05$

showed that the relative expression level of the gene showed an upwards trend with time during the differentiation of subcutaneous adipocytes, and the expression was highest at 108 h and significantly higher than 0 h ($P < 0.05$, Fig. 2D). The relative expression level of *FHL2* in intramuscular adipocytes showed an upward trend, and the expression level was the highest at 60 h ($P < 0.05$, Fig. 2E).

Effect of overexpression and silencing of *FHL2* on intramuscular adipocyte differentiation

Two bands matching the lengths of FHL2 and PCDNA3.1 appeared in the gel electropherogram (Supplementary Fig. S2). According to the analysis data, the overexpression of FHL2 was 300-fold compared to the control group (Fig. 3A). This indicates that the FHL2 overexpression vector was successfully constructed. Oil Red O staining and Bodipy staining showed a significant increase in subcutaneous adipocytes lipid aggregation and OD values after *FHL2* overexpression (Fig. 3B, C). In summary, *FHL2* promotes intramuscular adipocyte differentiation and secretion of lipid droplets. Preadipocytes differentiate into adipocytes and mature adipocytes are regulated by adipocyte markers and genes related to triglyceride synthesis. Therefore, we detected the mRNA levels of these genes through RT‑qPCR. The results showed

that *FHL2* overexpression significantly promoted the expression levels of *C/EBPβ* ($P < 0.05$), *PPARγ* ($P < 0.01$) and *SREBP* ($P < 0.05$), and inhibited the expression of *C/EBPα* ($P < 0.05$), *PREF-1* ($P < 0.01$) and *AP2* ($P < 0.05$, Fig. 3D). However, *FHL2* overexpression decreased the mRNA levels of triglyceride synthesis (TG) -related genes (Fig. 3E). Interestingly, *FHL2* increased the expression of *LPL* ($P < 0.01$) in subcutaneous adipocytes, but decreased *LPL* ($P < 0.05$) expression in intramuscular adipocytes.

For explore the mechanism of *FHL2* in adipocytes differentiation in more detail, we explored the effects of *FHL2* silencing on adipocytes. The results showed that *FHL2* silencing inhibited the expression of *FHL2* gene expression by approximately 50% (Fig. 3F). Bodipy and Oli Red O staining showed a significant decrease in the number of adipocytes and the degree of lipid droplet secretion after FHL2 silence in intramuscular adipocytes (Fig. 3G). The OD values were reduced by one-third (Fig. 3H). For the adipocyte differentiation marker genes, in the intramuscular adipocytes, the expression of *C/EBPα* ($P < 0.01$) and *PREF-1* ($P < 0.05$) significantly increased (Fig. 3I, J), while *C/EBPβ* ($P < 0.05$) and *PPARγ* ($P < 0.05$) expression decreased significantly. In the intramuscular adipocyte group, the expression of *ACC* ($P < 0.01$) and
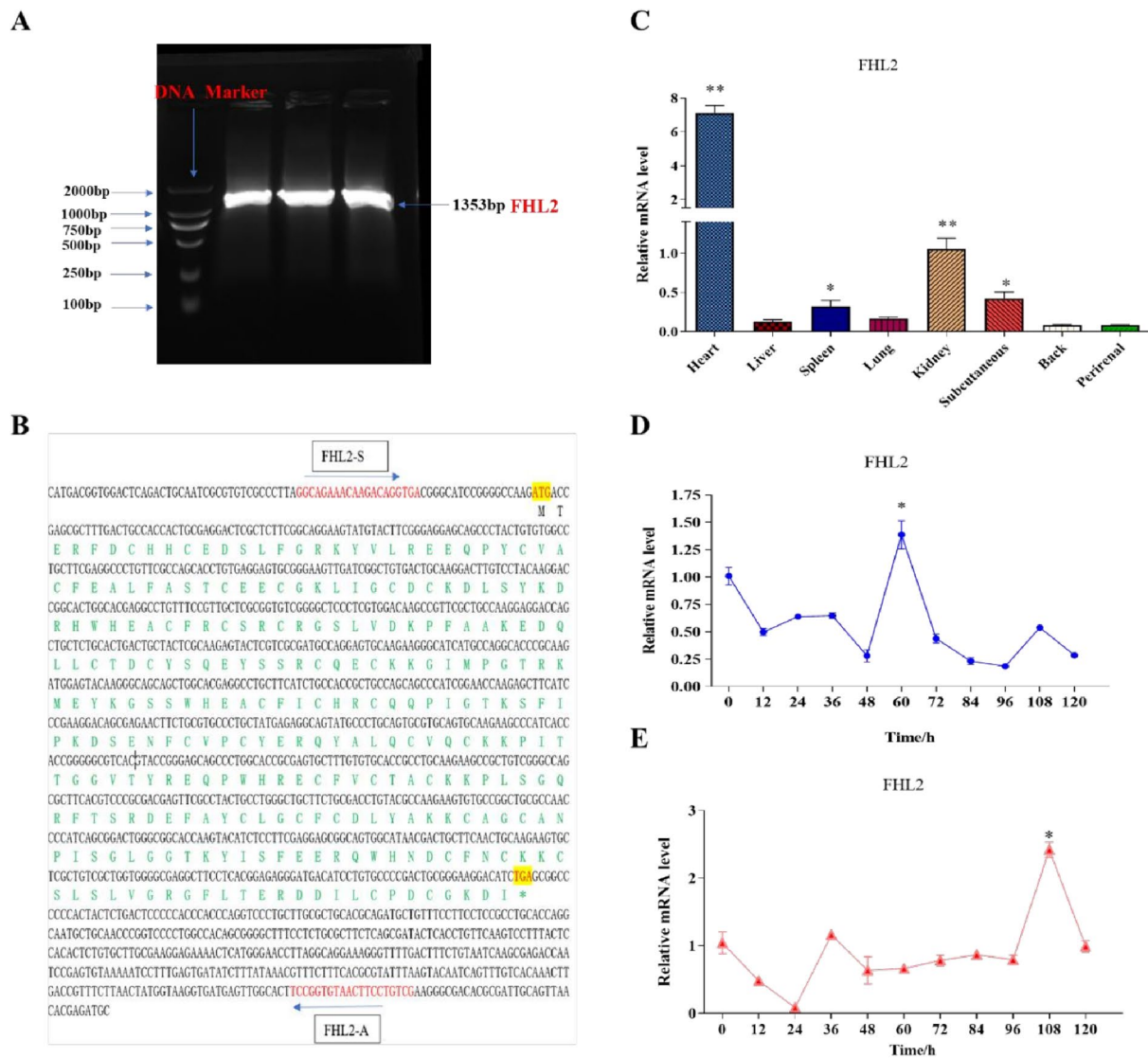
Fig. 2 Goat *FHL2* gene sequence analysis. **A** Amplification of *FHL2* gene in goat. DL 2000 DNA marker, *FHL2* target strip; **B** Sequence of nucleotide and derived amino acids Jian Zhou Da-er goat *FHL2* cDNA; **C** The expression of *FHL2* gene in different goat tissues."**"indicates that the difference is extremely significant difference between the data ($P < 0.01$),"*"indicate significant difference ($P < 0.05$); **D** The relative expression of *FHL2* during the differentiation of subcutaneous adipocytes. **E** The relative expression of *FHL2* during the differentiation of intramuscular adipocytes

LPL ($P < 0.05$) in the genes associated with triglyceride synthesis increased significantly.

Effect of overexpression and silencing of *FHL2* on subcutaneous adipocyte differentiation

In subcutaneous adipocytes, overexpression of *FHL2* was detected with effectiveness as it achieved 400-fold changes compared to the control group (Fig. 4A). Oil Red O and BODIPY staining showed a significant increase in the number of subcutaneous adipocytes and lipid droplet secretion. In addition, the OD value after *FHL2* overexpression was also increased significantly (Fig. 4B, C). In summary, the *FHL2* gene

promotes intramuscular adipocyte differentiation and lipid aggregation. Next, *FHL2* overexpression significantly promoted the expression of *PPARγ* ($P < 0.05$), *C/EBPβ* ($P < 0.05$), and *SREBP* ($P < 0.01$), and inhibited the expression of *CEBPα* ($P < 0.01$), *PREF-1* ($P < 0.01$), *AP2* ($P < 0.05$, Fig. 4D). However, *FHL2* overexpression increased the expression of the TG-related genes *ACC* ($P < 0.05$), *ADRP* ($P < 0.05$), and *LPL* ($P < 0.05$) and decreased the expression of *ATGL* and *GPAM* ($P < 0.05$, Fig. 4E).

In the subcutaneous adipocyte group, the silencing efficiency reached 50% (Fig. 4F), and a significant decrease in the number of subcutaneous adipocytes
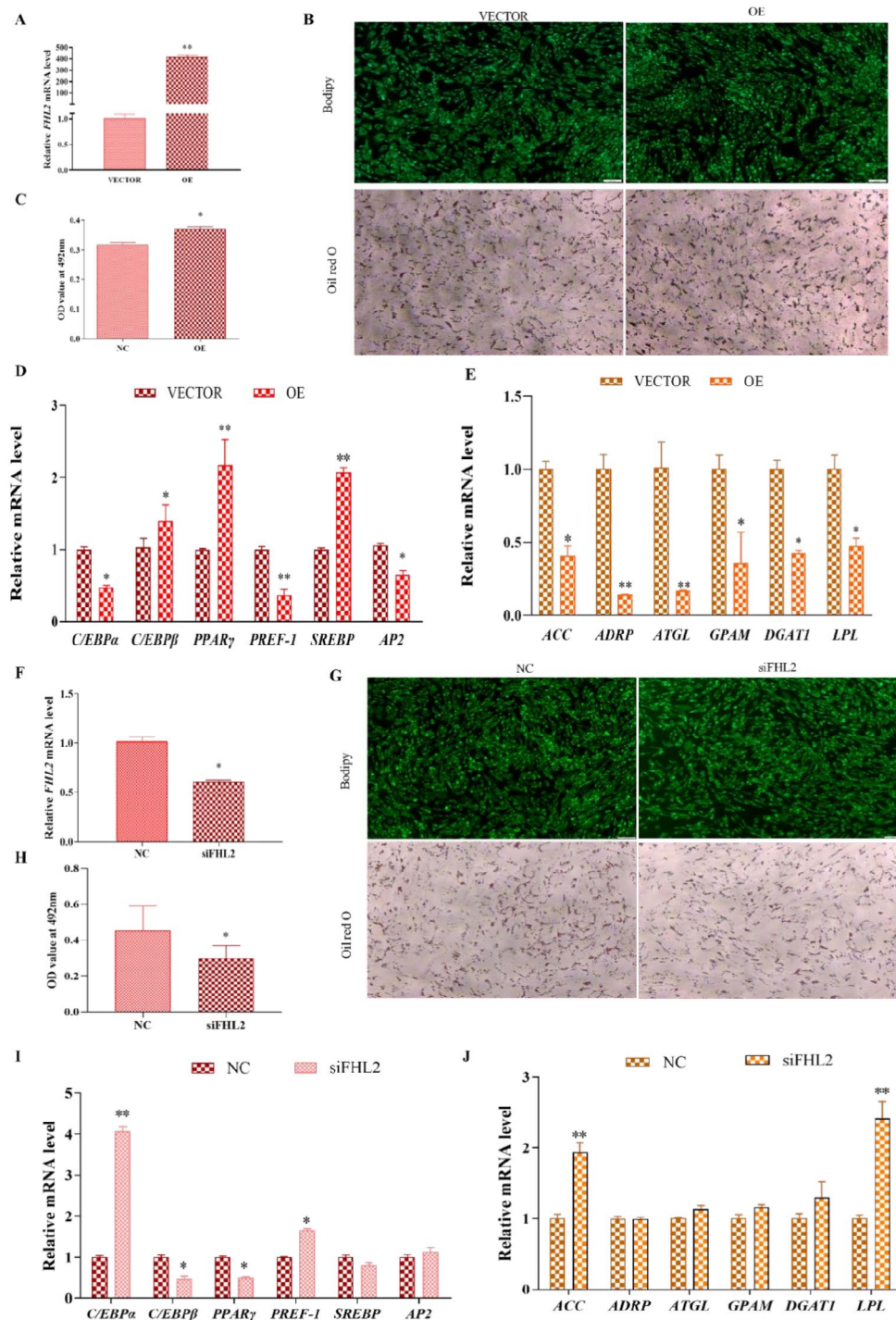
Fig. 3 The over-expression efficiency analysis of *FHL2* gene in intramuscular adipocytes. **A** The over-expression efficiency of *FHL2* was detected in mRNA level, $n = 5$; **B** Morphological observation of Bodipy staining and Oil Red O staining; **C** The OD value at 492 nm was detected by Oil Red O staining, $n = 8$; **D** Effects of *FHL2* overexpression in intramuscular adipocytes on differentiation marker genes; **E** Effects of *FHL2* overexpression in intramuscular adipocytes on triglyceride synthesis marker genes ($n = 6$). *UXT* was the internal reference gene to normalize the expression levels; **F** si*FHL2* efficiency of *FHL2* was detected in mRNA level, $n = 5$; **G** Morphological observation of Bodipy and Oil Red O staining; **H** The OD value was detected by Oil Red O staining, $n = 8$. "*" the difference is significant ($P < 0.05$); **I-J** Effect of silencing *FHL2* on intramuscular adipocyte differentiation marker genes and triglyceride synthases marker genes in the silencing *FHL2* and negative control. $n = 6$, *UXT* was the internal reference gene to normalize the expression levels. "**" the difference was extremely significant compared with the control group ($P < 0.01$), "*" the difference was significantly. Data were shown as Means ± SEM
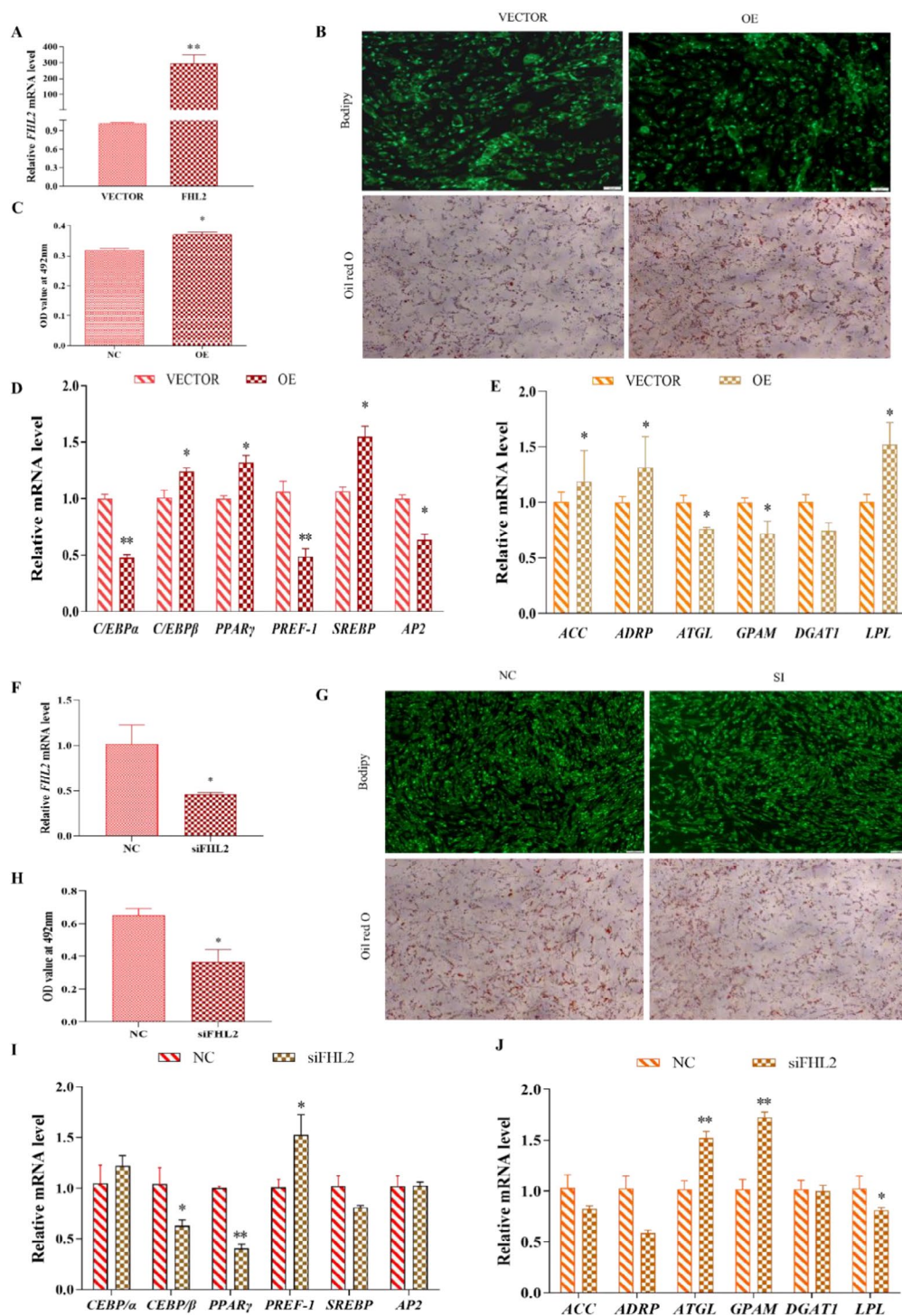
Fig. 4 The overexpression efficiency analysis of *FHL2* gene in subcutaneous adipocytes. **A** The over-expression efficiency of *FHL2* was detected in mRNA level, $n=5$; **B** Morphological observation of Bodipy and Oil Red O staining; **C** The OD value was detected by Oil Red O staining, $n=8$; **D** Effects of *FHL2* overexpression in subcutaneous adipocytes on differentiation marker genes; **E** Effects of *FHL2* overexpression in subcutaneous adipocytes on triglyceride synthesis marker genes; **F** The efficiency of silencing *FHL2* in subcutaneous adipocytes was detected at the mRNA level, $n=5$; **G** Morphological observation of Bodipy and Oil Red O staining; **H** The OD value was detected by Oil Red O staining, $n=8$; **I** Effects of silence of *FHL2* on adipocyte differentiation marker genes in subcutaneous adipocytes ($n=6$); **J** Effects of silencing *FHL2* in subcutaneous adipocytes on triglyceride synthesis marker genes. *UXT* was the internal reference gene to normalize the expression levels. "**" the difference was extremely significant ($P<0.01$), "*" the difference was significantly. Data were shown as Means $\pm$ SEM
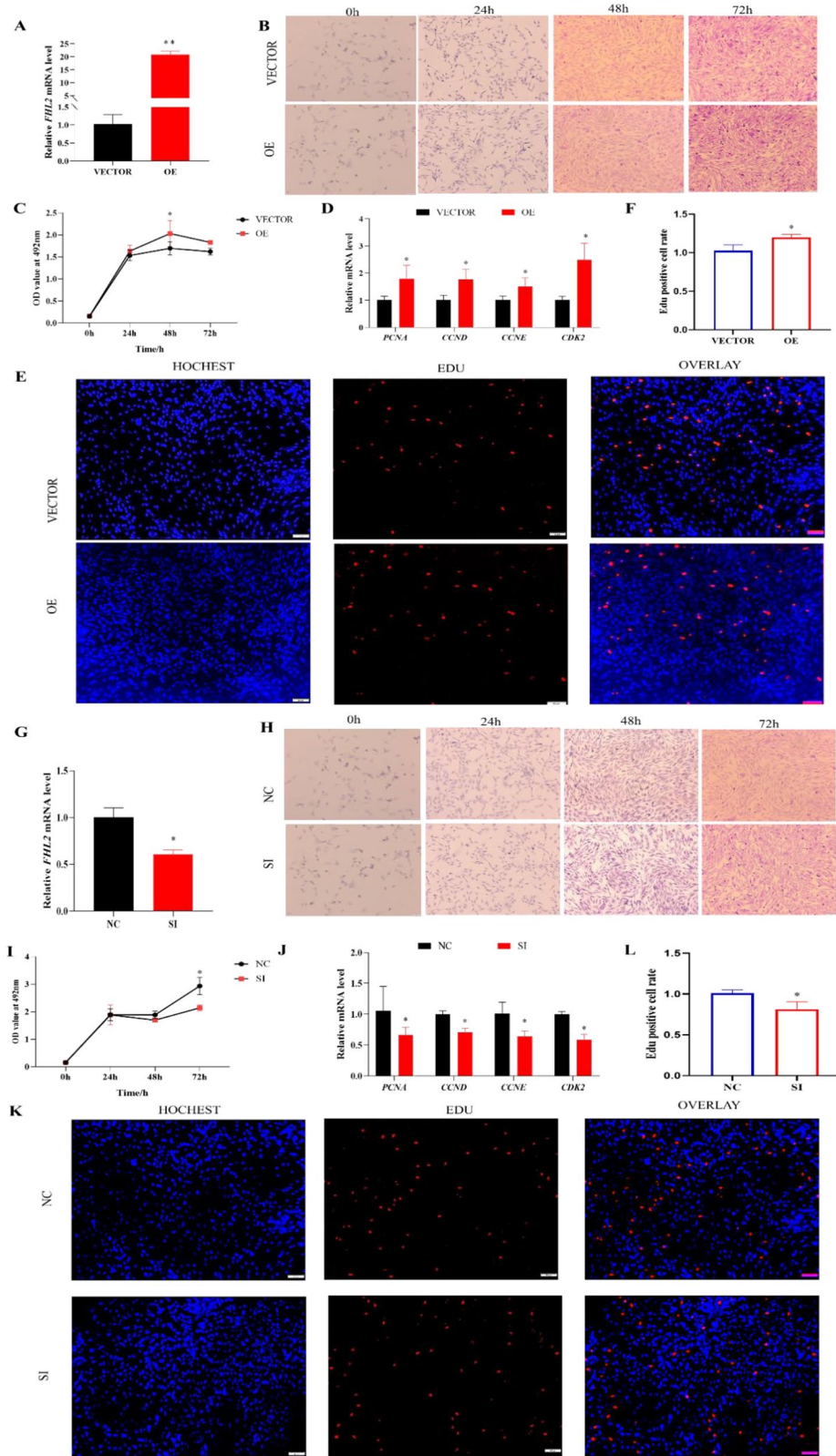
Fig. 5 (See legend on next page.)

Li *et al. BMC Genomics*   (2024) 25:850

Page 8 of 18

(See figure on previous page.)

Fig. 5 FHL2 promoted the proliferation of intramuscular adipocytes. **A** Analysis of *FHL2* overexpression efficiency; **B** Intramuscular adipocytes were stained using crystal violet staining to determine the effect of *FHL2* on adipocytes number after 0, 24, 48, and 72 h and photographed; **C** Intramuscular adipocytes proliferation was examined by MTT analysis; **D** RT-qPCR was used to detect the effects of *FHL2* on cell cycle genes, *PCNA*, *CCND*, *CCNE* and *CDK2*; **E** The proliferation capacity of the goat intramuscular adipocytes was examined by the EdU assay; **F** This image represents the results obtained by EdU after transfection overexpression *FHL2*; **G** Analysis of silent efficiency of *FHL2*; **H** The number of intramuscular adipocytes after transfection silencing *FHL2* at 0, 24, 48, and 72 h was determined by crystal violet staining; **I** Intramuscular adipocytes proliferation was examined by MTT analysis; **J** RT-qPCR was used to detect cell cycle genes, *PCNA*, *CCND*, *CCNE* and *CDK2* after 48 h transfection silencing *FHL2*; **K** EdU assay was carried out after transfection silencing *FHL2* for 48 h; **L** This image represents the results obtained by EdU after transfection silencing *FHL2*. "*" denotes $P < 0.05$, "**" indicates $P < 0.01$

and the secreted lipid droplets was observed under the microscope (Fig. 4G). In addition, the OD value was reduced by approximately one-third (Fig. 4H). In terms of adipocyte marker genes, the expression of *PREF-1* ($P < 0.05$) increased significantly, and the *CEBPβ* ($P < 0.05$) and *PPARγ* ($P < 0.01$) expression decreased significantly (Fig. 4I). In lipid marker genes, *ATGL* and *GPAM* expression increased significantly ($P < 0.01$), while the *LPL* expression decreased significantly ($P < 0.05$, Fig. 4J).

FHL2 promote the proliferation of goat intramuscular adipocytes

To explore the function of *FHL2* in the proliferation of intramuscular adipocytes, crystal violet staining, MTT, RT-qPCR and EdU staining were used to detect the proliferation of intramuscular adipocytes. RT-qPCR analysis showed that overexpression of *FHL2* was effective, as it achieved 20-fold changes in intramuscular adipocytes compared to the control group (Fig. 5A). After *FHL2* transfection for 24, 48, and 72 h, the number of adipocytes was observed by crystal violet staining. The results showed that the number of adipocytes in the *FHL2* overexpression group was greater than that in the vector group at any time (Fig. 5B). According to MTT data, the OD value at 490 nm was significantly increased in the *FHL2* overexpression group compared to the vector group (Fig. 5B), which was consistent with the trend of adipocyte number at 24, 48 and 72 h (Fig. 5C). The expression levels of *PCNA*, *CCND*, *CCNE* and *CDK2* were increased significantly ($P < 0.05$, Fig. 5D). Consistently, overexpression of *FHL2* significantly increased the positive rate of EdU in goat intramuscular adipocytes compared with the adipocytes transfected with vector ($P < 0.05$, Fig. 5E, F).

In the silencing experiment group, the expression of *FHL2* decreased significantly after silencing *FHL2* in intramuscular adipocytes ($P < 0.05$, Fig. 5G). Compared with the overexpression group, Si-FHL2 had the opposite effect on intramuscular adipocyte proliferation activity. The crystal violet staining results showed that Si-FHL2 significantly inhibited the number of goat intramuscular adipocytes at any time (Fig. 5H). In addition, MTT assay data showed that silencing *FHL2* significantly reduced the OD value at 490 nm (Fig. 5I),

which is proportional to the number of adipocytes at 24, 48 and 72 h. Furthermore, silencing *FHL2* significantly reduced the mRNA levels of cell proliferation-positively correlated markers (*CCNE*, *PCNA*, *CCND* and *CDK2*) ($P < 0.05$, Fig. 5J). The EdU results were consistent with the above trend, and the proliferation rate of intramuscular adipocytes was significantly reduced after silencing *FHL2* (Fig. 5K, L).

FHL2 promotes the proliferation of subcutaneous adipocytes

We used the same method as described in section 2.5 to investigate the effect of *FHL2* on the proliferation of subcutaneous adipocytes. RT-qPCR analysis showed that overexpression of *FHL2* was detected with effective, as it achieved 80-fold changes in subcutaneous adipocytes compared to the control group (Fig. 6A). The number of subcutaneous adipocytes after *FHL2* overexpression was significantly greater than that in the control group at any time (24, 48 and 72 h) by crystal violet staining (Fig. 6B). At the same time, the data obtained by MTT assay showed that the OD value overexpression of *FHL2* at OD value was significantly higher than that of the vector group, which was consistent with the trend of adipocytes number change at 24, 48 and 72 h (Fig. 6C). The expression levels of *PCNA* ($P < 0.05$), *CCNE* ($P < 0.05$) and *CDK2* ($P < 0.01$) increased after overexpression of *FHL2* (Fig. 6D). Compared to the intramuscular adipocyte group, the *CCND* expression did not change after *FHL2* overexpression, and the *CDK2* expression increased more significantly. Furthermore, the EdU assay was performed to detect proliferation and the proliferation rate of subcutaneous adipocytes was significantly increased after overexpression of *FHL2* (Fig. 6E, F).

FHL2 was silenced in goat subcutaneous adipocytes, and the results showed that the expression of *FHL2* significantly decreased after silencing *FHL2* ($P < 0.05$, Fig. 6G). Compared with the overexpression group, crystal violet staining results showed that Si-*FHL2* significantly reduced the number of subcutaneous adipocytes at any time (Fig. 6H). In addition, MTT assay data showed that silencing *FHL2* significantly reduced the OD value at 490 nm, which was proportional to the number of adipocytes at 24, 48 and 72 h (Fig. 6I). Furthermore, silencing *FHL2* significantly reduced

the mRNA levels of the cell proliferation positive correlated markers *PCNA* ($P < 0.05$), *CCNE* ($P < 0.05$) and *CDK2* ($P < 0.01$, Fig. 6j). The EdU assay results showed that the proliferation rate of subcutaneous adipocytes was significantly reduced ($P < 0.05$) compared with that of the control group after silencing *FHL2* (Fig. 6K, L).

FHL2 suppressed the apoptosis of intramuscular adipocytes

To explore the effects of *FHL2* on intramuscular adipocyte apoptosis, RT-qPCR was used to detect the mRNA expression levels of genes (*BCL2*, *P53* and *BAX*) associated with cell survival. The results showed that the expression levels of *BCL2* ($P < 0.05$) were significantly upregulated after overexpression of *FHL2* in intramuscular adipocytes (Fig. 7A), while *P53* ($P < 0.01$) and *BAX* ($P < 0.01$) were down-regulated. (Figure 7B and C). Finally, we also performed annexin V-FITC/PI staining assy. The apoptosis index in the group transfected with *FHL2* over-expression cells decreased significantly (Fig. 7D, E, $P < 0.05$).

In the *FHL2*-silenced group, the opposite trend was observed for FHL2 overexpression, and the mRNA expression level of BCL was significantly downregulated ($P < 0.01$, Fig. 7G). However, the mRNA expression of *BAX* and *P53* was upregulated ($P < 0.05$, Fig. 7F, H). In addition, the annexin V-FETC/PI staining assay showed that the silencing *FHL2-silenced* group had a significantly reduced cell survival rate and increased apoptosis (Fig. 7I, J).

FHL2 suppresses the apoptosis of subcutaneous adipocytes

The effect of *FHL2* on the apoptosis of subcutaneous adipocytes is large in the same way as described in section 3.5. After *FHL2* overexpression, *BAX* ($P < 0.01$, Fig. 8A) and *P53* ($P < 0.05$, Fig. 8B) expression levels decreased, and *BCL* expression levels increased ($P < 0.05$, Fig. 8C). The annexin V-FETC/PI staining assay showed that FHL2 overexpression significantly reduced the apoptosis rate and improved the cell survival rate ($P < 0.05$, Fig. 8D, E).

After silencing *FHL2*, the expression of *BAX* ($P < 0.05$, Fig. 8F) and *P53* ($P < 0.05$, Fig. 8G) increased, and the expression of *BCL* ($P < 0.01$) decreased (Fig. 8H). Through an annexin V-FITC/PI staining assay, it was found that the apoptosis rate of adipocytes increased significantly (Fig. 8I, J).

Discussion

The prevalence of obesity is rising globally, a series of diseases associated with obesity represent major public health issue [7–9]. Therefore, it is crucial to improve meat quality and human health by elucidating the molecular mechanisms of adipogenesis.

Previous reports showed that several *FHL2* were associated with adipocyte growth and development [19, 20]. In our study, *FHL2* was differentially expressed in intramuscular preadipocytes and mature intramuscular adipocytes in transcriptome sequencing analysis of intramuscular adipocytes 3 days after differentiation. FHL2 is found to be downregulated in mature adipocytes. Taken together, these data suggest that FHL2 may be associated with adipogenesis. The aim of this study was to investigate the exact role of *FHL2* in the development of subcutaneous adipocytes and intramuscular adipocytes.

In this study, we successfully cloned the FHL2 gene of goats and found that the nucleotides and amino acids of FHL2 were similar between goats and sheep respectively, indicating that goats are highly conserved between different species (Supplementary Fig. 3). Goat FHL2 protein maybe predominantly random coil. To further decipher the function of *FHL2*, the expression profile of FHL2 in goat tissue, as well as the temporal expression profile of *FHL2* in subcutaneous adipocyte differentiation and intramuscular adipocyte differentiation in goats were analyzed. Tissue expression profiles showed that FHL2 was widely expressed in goat tissues and highest in kidneys, and the study of Li Sirui et al. showed that *FHL2* has the highest expression in human and mouse kidneys, which was consistent with the results of this study [31]. Temporal expression profiles showed that *FHL2* expression changed during intramuscular and subcutaneous adipocyte differentiation, and the time points of the highest expression of *FHL2* were different in these two processes.

Previous studies have shown that FHL2 is positively correlated with fat hypertrophy, and loss of FHL2 protects mice from diet-induced obesity [32]. Adipocyte differentiation is a complex biological process that involves changes in cell structure and function [33] and is regulated by many transcription factors. Transcription factors such as *AP2*, *C/EBPα*, *C/EBPβ*, *SREBP*, *PREF-1* and *PPARγ*, are important in the process of adipocyte differentiation, among which *C/EBPβ* and *SREBP* promote the differentiation of adipocytes by activating the expression of *PPARγ* [34–37]. Bodipy and Oil red O staining revealed a significant increase in the number of adipocytes and lipid droplet secretion after *FHL2* overexpression, while the opposite trend occurred after *FHL2* silencing. In addition, the results showed that *FHL2* overexpression significantly promoted the expression of *PPARγ* and *C/EBPβ* in subcutaneous and intramuscular adipocytes, and the expression of *PREF-1* decreased after overexpression. At the molecular level, *FHL2* overexpression
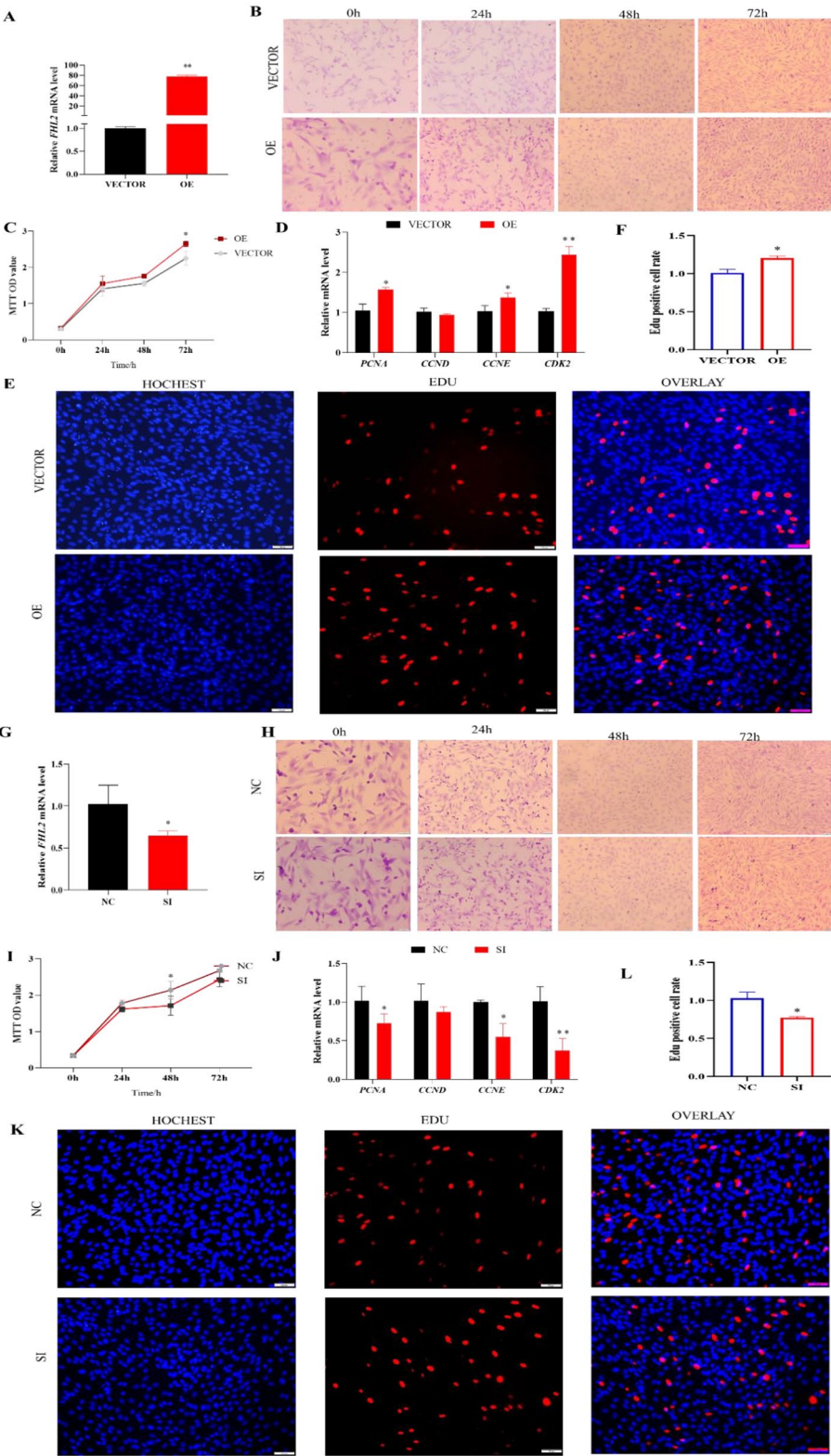
Fig. 6 (See legend on next page.)

(See figure on previous page.)

Fig. 6 FHL2 promoted the proliferation of subcutaneous adipocytes. **A** *FHL2* overexpression efficiency analysis; **B** Subcutaneous adipocytes were stained using crystal violet staining to determine the effect of *FHL2* on adipocytes number after 0, 24, 48, and 72 h and photographed; **C** Subcutaneous adipocytes proliferation was examined by MTT analysis; **D** RT-qPCR was used to detect the effects of *FHL2* on cell cycle genes, *PCNA*, *CCND*, *CCNE* and *CDK2* after overexpression in subcutaneous adipocytes; **E** The proliferation capacity of the goat subcutaneous adipocytes was examined by the EdU assay; **F** This image represents the results obtained by EdU after transfection overexpression *FHL2*; **G** Analysis of silent efficiency of *FHL2*; **H** The number of subcutaneous adipocytes after transfection silencing FHL2 at 0, 24, 48, and 72 h was determined by crystal violet staining; **I** Subcutaneous adipocytes proliferation was examined by MTT analysis; **J** RT-qPCR was used to detect cell cycle genes, *PCNA*, *CCND*, *CCNE* and *CDK2* after 48 h transfection silencing *FHL2*; **K** EdU assay was carried out after transfection silencing *FHL2* for 48 h; **L** This image represents the results obtained by EdU after transfection silencing *FHL2*. "*" denotes $P < 0.05$, "**" indicates $P < 0.01$

significantly promoted the expression of *PPARγ* and *C/EBPβ* in subcutaneous and intramuscular adipocytes, inhibited the expression of *PREF-1*, and showed a reverse trend after silencing with *FHL2*. Unlike this study, *FHL2* inhibits colon cancer cell line HT-29 cells and neuronal cell growth and differentiation [38, 39]. The results of this study show that *FHL2* promotes intramuscular and subcutaneous adipocyte differentiation in goats.

Studies have shown that *FHL2* promotes the proliferation of human colon cancer cells and breast cancer cells, and mouse smooth muscle cells and regulates the expression of cyclin *CCND* [40–42]. Cell proliferation is regulated by gene expression, such as *CCNE*, *PCNA*, *CCND*, and *CDK2*, which are all positive regulators of cell proliferation [43–46]. At the molecular level, overexpression of *FHL2* promotes the expression of *CCND*, *CCNE*, *CDK2*, and *PCNA* in intramuscular adipocytes and is inhibited after silencing *FHL2*. In subcutaneous adipocytes, it was found that *CCND* was not affected after overexpression of *FHL2*, and the expression of *CDK2* was more significant. A study reported that *FHL2* inhibits the proliferation of human hepatoma cells by inhibiting the expression of *CCND*, which is different from this study [47]. The above results indicate that *FHL2* promotes the proliferation of intramuscular and subcutaneous adipocytes.

Recent studies have shown that *FHL2* inhibited apoptosis in hepatoma cells, and enhancing *FHL2* expression promotes bone marrow progenitor cells to enter the cell cycle and increases the frequency of apoptosis in vivo by bone marrow cells. In addition, lncRNA DLX6-AS1 aggravates ovarian apoptosis by regulating miR-195-5p through sponging [48–50]. As a regulator of apoptosis, *BAX* induces cell damage leading to apoptosis, Bcl-2 encodes the outer mitochondrial membrane protein to inhibit cell apoptosis. As reports, the decrease of Bcl-2 is related with enhanced Bax signal, and *BCL* is known to inhibit *P53*-induced apoptosis [50, 51]. After overexpression of *FHL2* and then intramuscular adipocytes and subcutaneous adipocytes, the expression levels of *BCL* were upregulated, and the expression levels of *BAX* and *P53* were downregulated. In addition, the flow cytometry phenomenon showed that the apoptosis rate of adipocytes

after overexpression of *FHL2* was significantly lower than that of the control group, and the opposite phenomenon occurred after silencing *FHL2*. In summary, *FHL2* inhibits apoptosis of intramuscular and subcutaneous adipocytes.

Conclusion

This study shows *FHL2* may be a positive regulator of intramuscular and subcutaneous adipocyte differentiation and proliferation, and acts as a negative regulator of intramuscular and subcutaneous adipocyte apoptosis (Fig. 9).

Materials and methods
Cell culture

All experimental procedures were reviewed and approved by the Institutional Animal Care and Use Committee, Southwest Minzu University (Chengdu) (Number 20200120). Methods were performed according to the guidelines and regulations. Isolation and culture of goat intramuscular preadipocytes and subcutaneous adipocytes were performed as previously described [52, 53]. Cells stored in liquid nitrogen were thawed in a 37 ℃ water bath. Then add 5 mL of 10% fetal bovine serum (FBS, HyClone, Logan, America) with a total of 7 mL. And moved it to 10 mL tube and centrifuged at 289 g for 5 min. Discard the supernatant, leave the pallet and 5 mL FBS for mix well then cultured in petri dish. When the F3 cells grew to 80% confluence, 50 µmol/L of oleic acid (Sigma, Shanghai, China) was added to the culture medium to induce preadipocyte adipogenic differentiation.

Sequencing and differentially expressed gene screening

Qubit2.0 was used for preliminary quantification after the library was constructed. We diluted the library to 1 ng/ul, and then used Agilent 2100 to detect the insert size of the library. The qPCR was used to accurately quantify the effective concentration of the library (the effective concentration of the library > 2 nM), which can ensure the quality of the library. The constructed library was sequenced using the Illumina HiSeq-technique. The |log2FoldChange|>0 and *p* value < 0.05 were considered to indicate differential expressed.

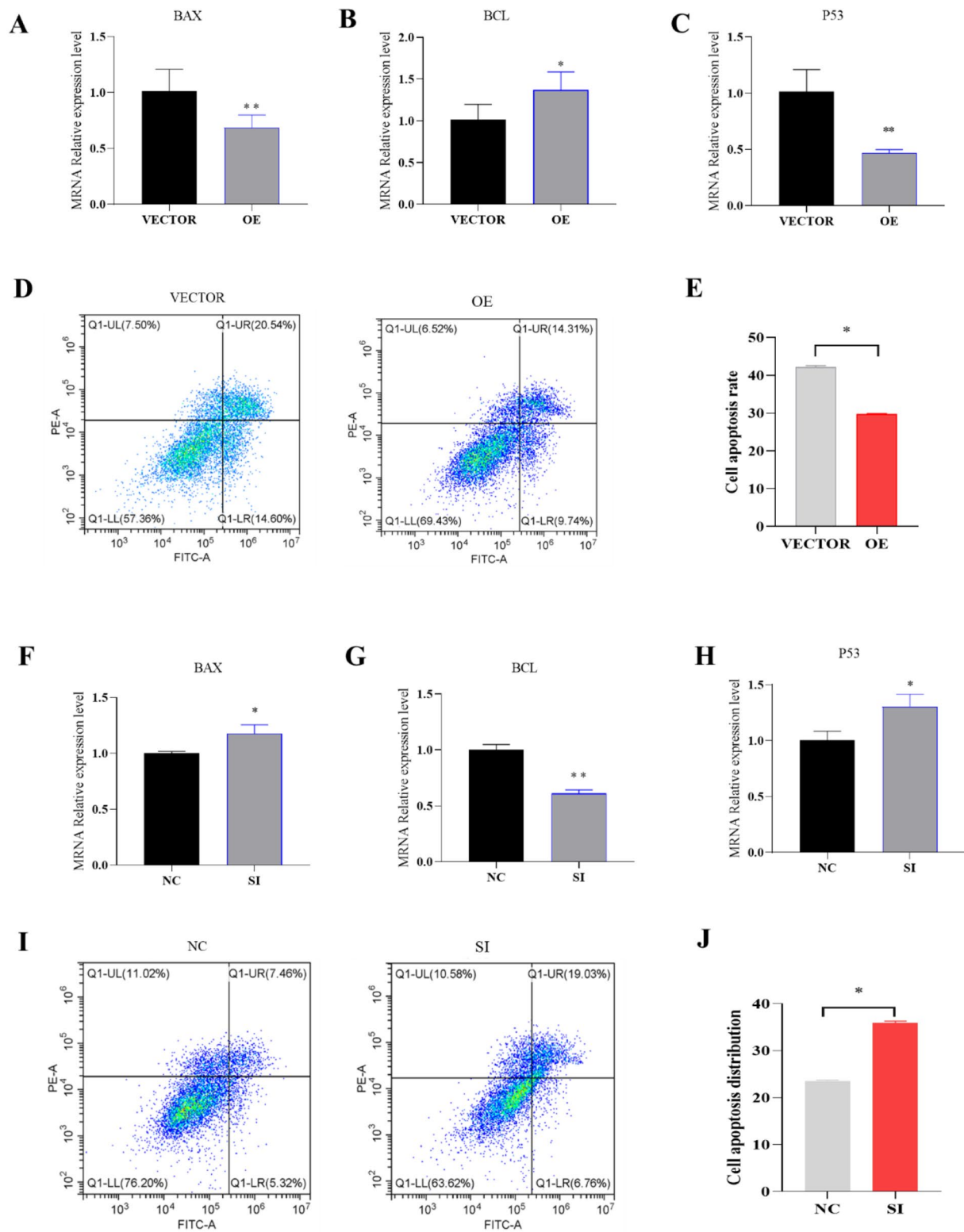Li *et al. BMC Genomics*   (2024) 25:850

Page 12 of 18

Fig. 7 FHL2 suppress intramuscular adipocytes apoptosis. **A-C** RT-qPCR detects the expression of the apoptosis marker genes expression level after *FHL2* overexpression; **D** Intramuscular adipocytes were transfected by *FHL2* overexpression and VECTOR, collected, and stained by Annexin V-FITC/PI. Intramuscular adipocytes apoptosis phase distribution was analyzed by flow cytometry; **E** Intramuscular adipocytes apoptosis index was analyzed between *FHL2* overexpression and VECTOR group; **F-H** RT-qPCR detects the expression of apoptosis relative genes after silencing *FHL2*; **I** Intramuscular adipocytes were transfected by silencing *FHL2* and NC, collected and stained by Annexin V-FITC/PI. Intramuscular adipocytes apoptosis phase distribution was analyzed by flow cytometry; **J** Intramuscular adipocytes apoptosis index was analyzed between silencing *FHL2* and NC group
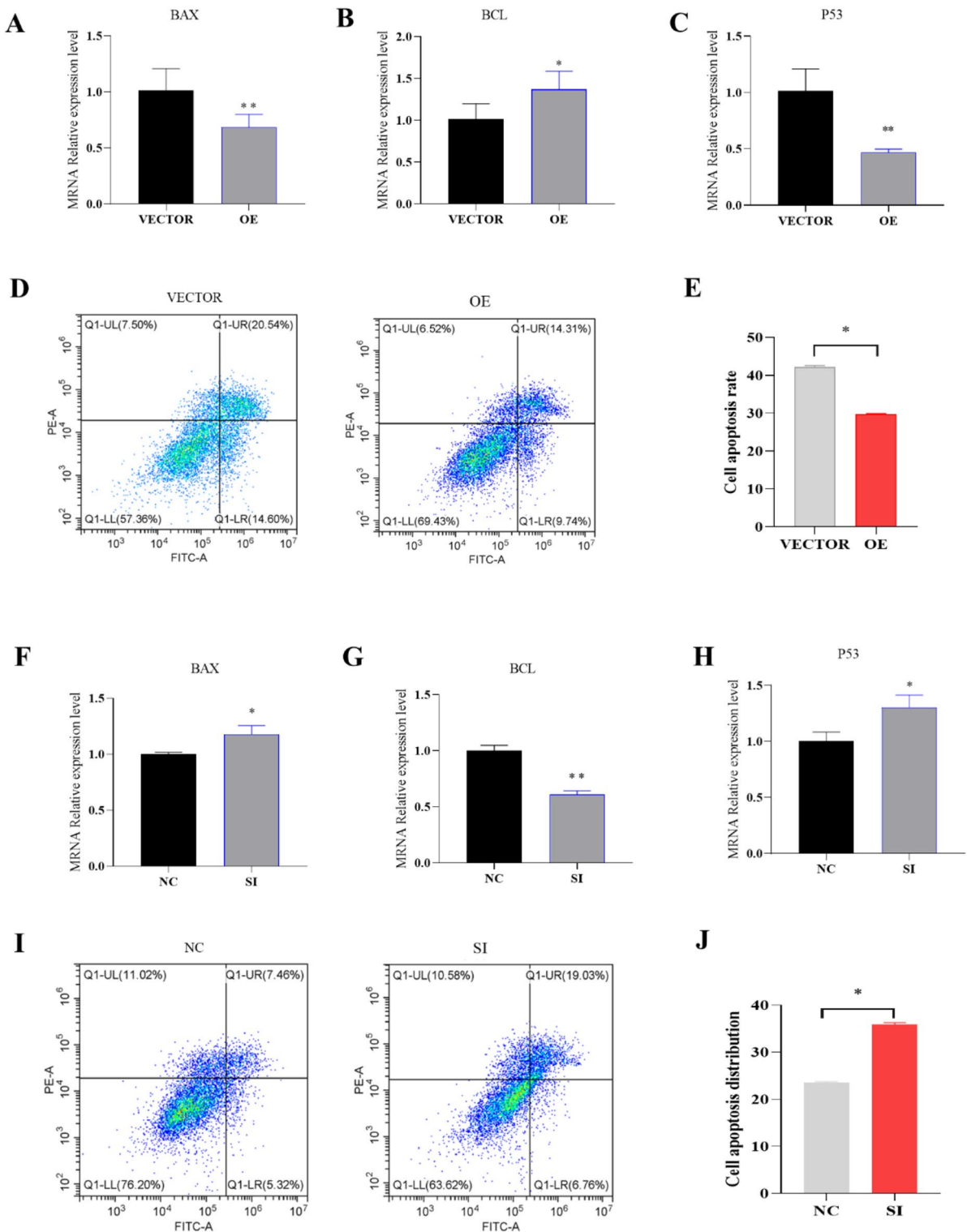
Li *et al. BMC Genomics*   (2024) 25:850

Page 13 of 18

Fig. 8 FHL2 suppress subcutaneous adipocytes apoptosis. **A-C** RT-qPCR detects the expression of the apoptosis marker genes after silencing *FHL2*; **D** Subcutaneous adipocytes were transfected by *FHL2* overexpression and VECTOR, collected, and stained by Annexin V-FITC/PI. Subcutaneous adipocytes apoptosis phase distribution was analyzed by flow cytometry; **E** Subcutaneous adipocytes apoptosis index was analyzed between *FHL2* overexpression and VECTOR group; **F-H** RT-qPCR detects the expression of apoptosis marker genes after silencing *FHL2*; **I** Subcutaneous adipocytes were transfected by silencing *FHL2* and NC, collected and stained by Annexin V-FITC/PI. Subcutaneous adipocytes apoptosis phase distribution was analyzed by flow cytometry; **J** Subcutaneous adipocytes apoptosis index was analyzed between silencing *FHL2* and NC group
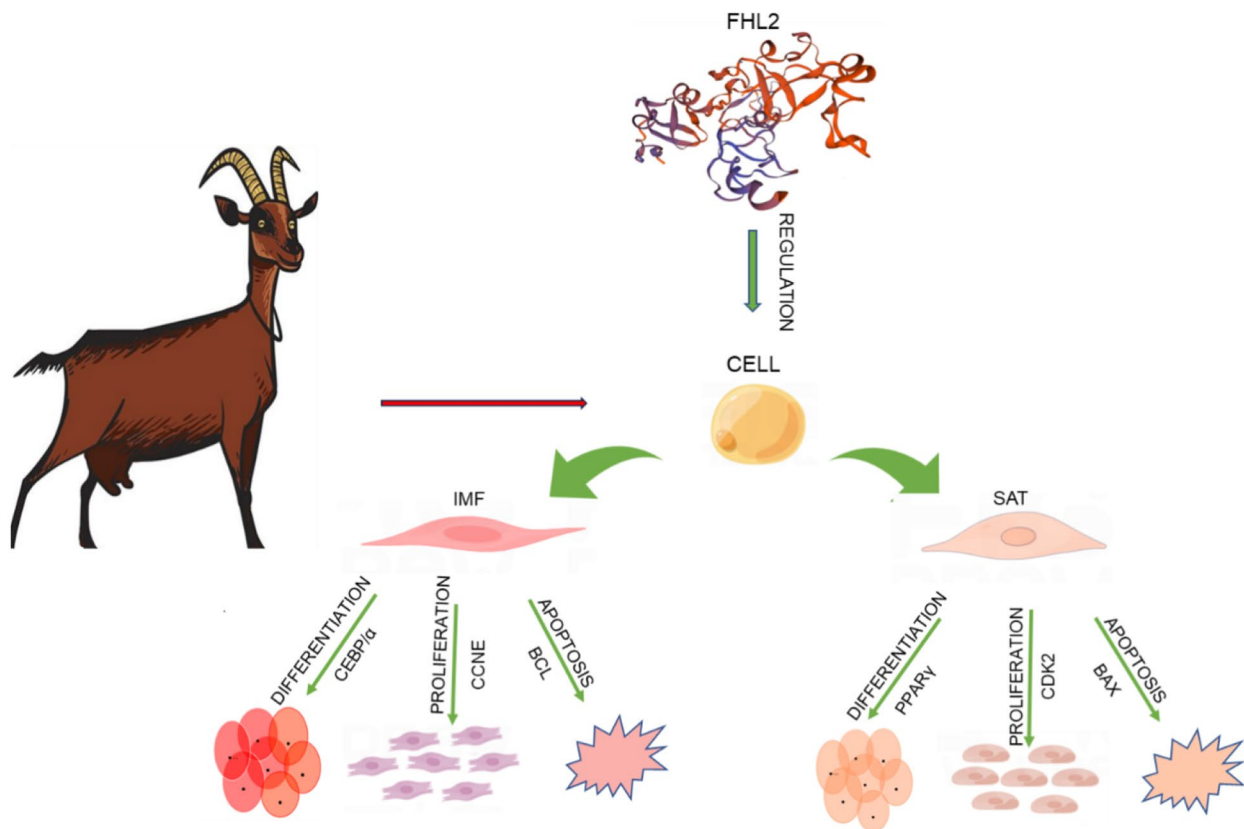
Fig. 9 Effects of gene *FHL2* on the development of subcutaneous and intramuscular adipocytes in goats

Animals

Jian-Zhou Da-er goats (*n* = 3) were selected as test animal. Tissue samples such as heart, liver, spleen, lung, kidney, subcutaneous, back and periend. The samples were washed with DEPC (diethypyrocarbonate) water quickly loaded into Rase-free compere and stored in liquid nitrogen. First strand of cDNA was synthesized by the Revert Aid First strand cDNA synthesis Kit (Therma, Massachusetts, America).

FHL2 gene cloning

According to the predicted sequences of goat *FHl2* mRNA (GenBack accession number XM-018054974.1). The primer pair (Table 1) was designed using Primer Premier 5.0 software. The PCR system contained 1.1 x T3 super PCR mix 22 μL, cDNA (10 μmol/L) 1 μL, FHL2-S (10 μmol/L) 1 μL, and FHL2-A (10 μmol/L) 1 μL. The PCR procedure, included pre-degeneration (98 ℃, 3 min), all of degeneration (98 ℃, 10 s), annealing (60 ℃, 10 s) and extension (72 ℃, 20 s) 35cycles. Final extension (72 ℃, 2 min), preserving at 4 ℃. The destination strand was recycled via recovery kit (Takara, Tokyo, Japan). Strands were ligated into the 007 vs. vector (Tsinke, Beijing, China) and sequenced by Tsingke Biotechnology. Co. Ltd.

Expression patterns of FHL2 gene in goat tissues and subcutaneous and intramuscular adipocyte adipogenesis
Expression patterns of the FHL2 gene in goat tissues

cDNA (heart, liver, spleen, lung, kidney, subcutaneous fat, back, perirenal) from goats was used to perform RT-qPCR to detect gene expression levels. RT-qPCR primers (Table 1) were designed according to the *FHL2* gene CDS region obtained from cloning. Detection of FHL2 gene expression levels in different goat tissues. 10 μL PCR mixture: D-FHL2-S (10 μmol/μL) 0.5 μL, D-Fhl2-A (10 μmol/μL) 0.5 μL, TB Green $^{TM\ premix}$ 2×5 μL, ddH$_2$O 3.5 μL and cDNA 0.5 μL. Procedure: Pre-degeneration (95 ℃, 3 s), all of degeneration (95 ℃, 10 s), annealing (58 ℃, 10 s), extension (72 ℃ 15 s), 38 cycles. Four duplicates per tissue.

Expression patterns of the FHL2 gene in goat subcutaneous and intramuscular adipocyte adipogenesis

The expression level of *FHL2* in subcutaneous and intramuscular adipocytes at different stages of differentiation (0, 12, 24, 36, 48, 60, 72, 84, 96, 108 and 120 h) was detected in the same way as mentioned in 1.4 above. qPCR was used to detect the expression pattern of the *FHL2* gene in the adipocytes that were induced to differentiate from 0 h to 120 h by oleic acid.

Construction of the FHL2 overexpression vector

We used DNAMAN to find the restriction enzyme of *FHL2* (NEHI, KPNI two enzymes used to construct an overexpression vector) based on the *FHL2* sequence of Jian Zhou Da-er goat, designed the subcloning primers OE-FHL2-S (TAGCATGACCGAG CGCTTTGAC, start codon is ATG, GCTAGC is the restriction site of NEHI) and OE-FHL2 (GGGGTA CCTCAGAGATGTCCTTCCCGCA, the restriction site of KPNI is GGTACC AGT is the stop codon). The goat *FHL2* plasmid was used as a template to amplify its CDS. Then we used PCDNA3.1 (stored by key of Qinghai Tibetan Plateau Animal Genetic Resource Reservation and Utilization Ministry of Education, Southwest Minzu University) as a vector. The second digestion was performed with the CDS vector by KPNI (Thermo, Massachusetts, America) and NEHI (Thermo, Massachusetts, America) at 37 ℃ for 30 min, followed by purification and ligation with T4 ligase (Takara, Tokyo, Japan) in a 16 ℃ water bath for 16 h. Finally, the recombinant vector was identified by enzyme digestion and detected by gel- electrophoresis, and sequencing.

Oil Red O and BODIPY staining

Cells were washed 3 times with phosphate-buffered saline (PBS), then fixed it in 4% formaldehyde for 30 min, washed 3 times with PBS, and stained with Oil Red O for 1 h (Solarbio, Beijing, China), and then washed three times with polyester PBS and moistened, then photographed with an epifluorescence microscope equipped (Olympus IX-73, Tokyo, Japan). Oil Red O dye was extracted with 100% isopropanol, and the Oil Red O signal was quantified by measuring the absorbance at 490 nm to determine the extent of lipid drop accumulation. Fixed cells were stained with BODIPY solution for 20 min, washed three times and moistened with PBS for imaging by microscope.

MTT assay

MTT assay was used to detect intramuscular and subcutaneous adipocyte proliferation in goats. Intramuscular and subcutaneous preadipocytes were seeded in 96-well plates at a density of 4×10^3 cells per well. After 0, 24, 48 and 72 h of adipocyte culture, 10 μL of MTT reagent (Solarbio, Beijing, China) was added to each well, away from light, and then the adipocytes were incubated with 5% CO_2 at 37 °C for 3.5 h. Finally, absorbance was measured at a wavelength of 490 nm using an enzyme-labelled instrument (PEI OU, Shanghai, China).

Cell proliferation and apoptosis assay
EdU proliferation assay
The intramuscular and subcutaneous preadipocyte abilities in goats were measured by an EdU incorporation assay (Beyotime, Shanghai, China). First, goat intramuscular and subcutaneous adipocytes were seeded in 24-well plates and then transfected when confluency reached 60%. After 48 h of transfection, goat intramuscular and subcutaneous adipocytes were stained with 50 μmol/μL EdU solution for 2 h, fixed with 4% paraformaldehyde for 30 min, and infiltrated with 0.3% Triton X-100 for 15 min. Cells were then incubated with the click-reaction mix provided with the EdU staining kit for 20 min and stained with DAPI for 20 min. Finally, adipocytes were photographed by a fluorescence microscope (Olympus, Tokyo, Japan).

Cell apoptosis assay
The original culture medium was aspirated and moved to a centrifuge tube, the cells were rinsed with PBS, and the waste solution was discarded. Add 1 mL of EDTA-free pancreatic enzyme for digestion, wait for the cells to be separated, add the original culture medium to terminate the digestion, and collect the cells. Centrifuge at 289 g for 5 min, aspirate the supernatant, wash twice with PBS, collect the cell pellet, resuspend the cells with a 500 μL binding buffer, add 5 μL ANNEXIN V to blow well, and then add 5 μL PI to mix well. The reaction at room temperature is protected from light for 15 min, and the machine is detected and analysed.

RT-qPCR, RNA-seq data verification and data analysis
RT-qPCR
Total RNA (1 μg) was used for reverse transcription and mRNA reverse transcription, and the obtained cDNA was used as a template for qPCR to detect expression levels, which were randomly selected from differentially expressed mRNAs to verify the accuracy of the RNA-Seq results. In addition, we obtained cDNA from goat tissues and cultured cells and detected the expression levels of *FHL2*. To normalize the level of mRNA in tissues and adipocytes, a ubiquitously expressed gene (*UXT*) was selected as an internal reference gene. In addition, the expression of differentiation marker genes such as *C/EBPα*, *C/EBPβ*, *PPARγ*, *PREF-1*, *SREBP* and *AP2* were detected. The sequences of the primers are shown in the Table 1. RT−qPCR was carried out with a Bio Rad Real-Time PCR system. Data were analysed using the comparative Ct method ($2^{-\Delta\Delta Ct}$).

Statistical analysis of data
GraphPad 8.0 software was used for significance analysis and multiple comparison. Data are expressed as the

Li *et al. BMC Genomics*   (2024) 25:850

Page 16 of 18

Table 1 The information of primers

Gene name	sequence	Purpose	Length	Tm
FHL2	S: AGGCAGAAACAAGACAGGTGA	PCR	1353bp	58℃
	A: CGACAGGAAGTTACACCGGA			
D-FHL2	S: GCACCCGCAAGATGGAGTA	RT-qPCR	180bp	60℃
	A: TCGGGATGAAGCTCTTGGTT			
UXT	S: GCAAGTGGATTTGGGCTGTAAC	RT-qPCR	180bp	60℃
	A: ATGGAGTCCTTGGTGAGGTTGT			
C/EBPα	S: CTCCGGATCTCAAGACTGCC	RT-qPCR	136bp	60℃
	A: CCCCTCATCTTAGACGCACC			
C/EBPβ	S: CAACCTGGAGACGCAGCACAAG	RT-qPCR	204bp	60℃
	A: GCTTGAACAAGTTCCGCAGGGT			
PPARγ	S: AAGCGTCAGGGTTCCACTATG	RT-qPCR	197bp	60℃
	A: GAACCTGATGGCGTTATGAGAC			
PREF-1	S: CCTGAAAATGGATTCTGCGACG	RT-qPCR	255bp	60℃
	A: GACACAGGAGCACTCGTACTG			
SREBP	S: AACATCTGTTGGAGCGAGCA	RT-qPCR	134bp	60℃
	A: TCCAGCCATATCCGAACAGC			
AP2	S: TGAAGTCACTCCAGATGACAG	RT-qPCR	143bp	60℃
	A: TGACACATTCCAGCACCAG			
ACC	S: GGAGACAAACAGGGACCATT	RT-qPCR	180bp	60℃
	A: ATCAGGGACTGCCGAAAC			
ADRP	S: TACGATGATACAGATGAATCCCAC	RT-qPCR	170bp	60℃
	A: CAGCATTGCGAAGCACAGAGT			
ATGL	S: GGTGCCAATATCATCGAGGT	RT-qPCR	125bp	60℃
	A: CACACCCGTGGCAGTCAG			
GPAM	S: GGAGCAAGCATTGTTGCCAG	RT-qPCR	135bp	60℃
	A: CAATCAGTCTTCGGCGGGAT			
DGAT1	S: CCACTGGGACCTGAGGTGTC	RT-qPCR	140bp	60℃
	A: GCATCACCACACACCAATTCA			
LPL	S: TCCTGGAGTGACGGAATCTGT	RT-qPCR	114bp	60℃
	A: GACAGCCAGTCCACCACGAT			
PCNA	S: TTTGAGGCACGCCTGATCC	RT-qPCR	172bp	60℃
	A: GGAGACGTGAGACGAGTCCAT			
CCND	S; TAGGCCCTCAGCCTCACTC	RT-qPCR	80bp	60℃
	A: CCACCCCTGGGATAAAGCAC			
CCNE	S: CTTGCAGTGAGTGACGTAGAC	RT-qPCR	94bp	60
	A: CCAGTTGTCGGAGATAAGCATAG			
CDK2	S; CAAAGCCAAGCACGTAGAGAC	RT-qPCR	141bp	60
	A: TGCACCACATATTGACTGTCC			
BAX	S: TGAAGACAGGGGCCTTTTTG	RT-qPCR	140bp	60
	A: AATTCGCCGGAGACACTCG			
BCL	S: GACTTCTCTCGGCGCTACC	RT-qPCR	198bp	60
	A: CACATGACCCCTCCGAACTC			
P53	S: CAACAAATGCTGGCTACTAAGGA	RT-qPCR	168bp	60
	A: CACGAGTTTTCCGTTGCTCA			

mean±SEM. *P*<0.05 was defined as the significance threshold. RT-qPCR data through the 2-$^{-\Delta\Delta Ct}$ method analysis. "b", and "*" indicate that the difference was significant *(P*<0.05), and "a, **" indicate that the difference was extremely significant.

Abbreviations

ACC	Acetyl-CoA carboxylase
ADRP	Adipose differentiation-related protein
ANNEXIN V	The method to detect the cell apoptosis
AP2	APETALA-2-Like transcription factor gene
ATGL	Fat triglyceride lipase
BAX	Bcl-2-associated X protein
BCL	B-cell lymphoma
C/EBPβ	CCAT enhancer binding proteinβ
CCND	Cyclin D1
CCNE	Cyclin E1
CDK2	Cyclin-Dependent Kinases
DEPC	Diethypyrocarbonate
DGAT	Diglyceryl acyltransferase

Li *et al. BMC Genomics*   (2024) 25:850

Page 17 of 18

E4F1	E4 transcription factor
EdU	The method to detect the cell ability
FHL2	Four and half LIM protein
GPAM	Glycerol-3-phosphate acyltransferase
LPL	Lipoprotein lipase
MTT	The method used in this experiment to detect cell viability
P21	Cyclin-dependent kinase inhibitor 1 A
P27	Tumor suppressor 27
P53	Tumor suppressor 53
PCNA	Proliferating cell nuclear antigen
PI	The method for stain cell
PPARγ	Peroxisome proliferator activated receptory
PREF-1	Preadipocyte Factor 1
RT-qPCR	Real time quantitative polymerase chain reaction
SKI	Protein (SKI)
SREBP-1	Sterol regulating element binding protein isoform 1

Supplementary Information

The online version contains supplementary material available at https://doi.org/10.1186/s12864-024-10755-8.

Supplementary Material 1

Data availability
The raw data supporting the results of this study may be obtained from the corresponding authors upon reasonable request. The name of the database is Open science framework, which can be obtained through this link https://doi.org/10.17605/OSF.IO/N7M2S.

Declarations

Ethics approval and consent to participate
We purchased one year old male Jian-Zhou Da-er goats (*n* = 3) from Jianyang Tian Di Animal Husbandry Co., Ltd. (Sichuan, China) and we obtained the informed consent from the owner for the use of animals. And the experimental animals were injected barbiturate injection into the intraperitoneal cavity at a dose of 100 mg/kg, then bled to death. The carcasses are temporarily stored in freezer and then handed over to a professional solid waste disposal company for unified disposal. The experiment in this study were complied with the requirements of the directory of the Ethical Treatment of Experimental Animals of China. The animal study was reviewed and approved by Animal Experimental Ethical Inspection Committee of Southwest Minzu University (Chengdu, Sichuan, China), and all the experiment were performed under the requirement No. 2020-1-20. All animal experimental protocol has been carried out in accordance with relevant guidelines and regulations. All methods are reported in accord-ance with ARRIVE guidelines for the reporting of animal experiments.

Consent for publication
Not applicable.

Competing interests
The authors declare no competing interests.

References
1. Ottaviani E, Malagoli D, Franceschi C. The evolution of the adipose tissue: a neglected enigma. Gen Comp Endocrinol. 2011;174(1):1–4.
2. Coelho M, Oliveira T, Fernandes R. Biochemistry of adipose tissue: an endocrine organ. Arch Med Sci. 2013;9(2):191–200.
3. Halberg N, Wernstedt-Asterholm I, Scherer PE. The adipocyte as an endocrine cell. Endocrinol Metab Clin North Am. 2008;37(3):753–xi.
4. Liu R, Liu X, Bai X, Xiao C, Dong Y. A study of the regulatory mechanism of the CB1/PPARγ2/PLIN1/HSL pathway for fat metabolism in cattle. Front Genet. 2021;12:631187.
5. Anderson F, Pannier L, Pethick DW, Gardner GE. Intramuscular fat in lamb muscle and the impact of selection for improved carcass lean meat yield. Animal. 2015;9(6):1081–90.
6. Wang Y, Zhang Y, Su X, Wang H, Yang W, Zan L. Cooperative and independent functions of the miR-23a ~ 27a ~ 24–2 cluster in bovine adipocyte adipogenesis. Int J Mol Sci. 2018;19(12):3957.
7. Arner P, Kulyté A. MicroRNA regulatory networks in human adipose tissue and obesity. Nat Rev Endocrinol. 2015;11(5):276–88.
8. Hausman DB, DiGirolamo M, Bartness TJ, Hausman GJ, Martin RJ. The biology of white adipocyte proliferation. Obes Rev. 2001;2(4):239–54.
9. Hilton C, Neville MJ, Karpe F. MicroRNAs in adipose tissue: their role in adipogenesis and obesity. Int J Obes (Lond). 2013;37(3):325–32.
10. Li M, Sun X, Cai H, Sun Y, Plath M, Li C, Lan X, Lei C, Lin F, Bai Y, Chen H. Long non-coding RNA ADNCR suppresses adipogenic differentiation by targeting miR-204. Biochim Biophys Acta. 2016;1859(7):871–82.
11. Park CY, Han SN. The role of vitamin D in adipose tissue biology: adipocyte differentiation, energy metabolism, and inflammation. J Lipid Atheroscler. 2021;10(2):130–44.
12. Chu PH, Ruiz-Lozano P, Zhou Q, Cai C, Chen J. Expression patterns of FHL/SLIM family members suggest important functional roles in skeletal muscle and cardiovascular system. Mech Dev. 2000;95(1–2):259–65.
13. Zhou R, Li S, Liu J, Wu H, Yao G, Sun Y, Chen ZJ, Li W, Du Y. Up-regulated FHL2 inhibits ovulation through interacting with androgen receptor and ERK1/2 in polycystic ovary syndrome. EBioMedicine. 2020;52:102635.
14. van de Pol V, Vos M, DeRuiter MC, Goumans MJ, de Vries CJM, Kurakula K. LIM-only protein FHL2 attenuates inflammation in vascular smooth muscle cells through inhibition of the NFκB pathway. Vascul Pharmacol. 2020;125–126:106634.
15. Cai T, Sun D, Duan Y, Qiu Y, Dai C, Yang J, He W. FHL2 promotes tubular epithelial-to-mesenchymal transition through modulating β-catenin signalling. J Cell Mol Med. 2018;22(3):1684–95.
16. Zhu Y, Li P, Dan X, Kang X, Ma Y, Shi Y. miR-377 inhibits proliferation and differentiation of bovine skeletal muscle satellite cells by targeting FHL2. Genes (Basel). 2022;13(6):947.
17. Wang GF, Niu X, Liu H, Dong Q, Yao Y, Wang D, Liu X, Cao C. c-Abl kinase regulates cell proliferation and ionizing radiation-induced G2/M arrest via phosphorylation of FHL2. FEBS Open Bio. 2021;11(6):1731–8.
18. Lu Y, Cai G, Cui S, Geng W, Chen D, Wen J, Zhang Y, Zhang F, Xie Y, Fu B, Chen X. FHL2-driven molecular network mediated Septin2 knockdown inducing apoptosis in mesangial cell. Proteomics. 2014;14(21–22):2485-97. https://doi.org/10.1002/pmic.201400252. Epub 2014 Sep 22. PMID: 25103794.
19. Habibe JJ, Clemente-Olivo MP, Scheithauer TPM, Rampanelli E, Herrema H, Vos M, Mieremet A, Nieuwdorp M, van Raalte DH, Eringa EC, de Vries CJM. Glucose-mediated insulin secretion is improved in FHL2-deficient mice and elevated FHL2 expression in humans is associated with type 2 diabetes. Diabetologia. 2022;65(10):1721–33.
20. Clemente-Olivo MP, Habibe JJ, Vos M, Ottenhoff R, Jongejan A, Herrema H, Zelcer N, Kooijman S, Rensen PCN, van Raalte DH, Nieuwdorp M, Eringa EC, de Vries CJ. Four-and-a-half LIM domain protein 2 (FHL2) deficiency protects mice from diet-induced obesity and high FHL2 expression marks human obesity. Metabolism. 2021;121:154815.
21. Labalette C, Nouët Y, Sobczak-Thepot J, Armengol C, Levillayer F, Gendron MC, Renard CA, Regnault B, Chen J, Buendia MA, Wei Y. The LIM-only protein FHL2 regulates cyclin D1 expression and cell proliferation. J Biol Chem. 2008;283(22):15201–8.

Li *et al. BMC Genomics*   (2024) 25:850

Page 18 of 18

22. Paul C, Lacroix M, Iankova I, Julien E, Schäfer BW, Labalette C, Wei Y, Le Cam A, Le Cam L, Sardet C. The LIM-only protein FHL2 is a negative regulator of E4F1. Oncogene. 2006;25(40):5475–84.

23. Lai CF, Bai S, Uthgenannt BA, Halstead LR, McLoughlin P, Schafer BW, Chu PH, Chen J, Otey CA, Cao X, Cheng SL. Four and half lim protein 2 (FHL2) stimulates osteoblast differentiation. J Bone Min Res. 2006;21(1):17–28.

24. Lu Y, Cai G, Cui S, Geng W, Chen D, Wen J, Zhang Y, Zhang F, Xie Y, Fu B, Chen X. FHL2-driven molecular network mediated Septin2 knockdown inducing apoptosis in mesangial cell. Proteomics. 2014;14(21–22):2485–97.

25. Scholl FA, McLoughlin P, Ehler E, de Giovanni C, Schäfer BW. DRAL is a p53-responsive gene whose four and a half LIM domain protein product induces apoptosis. J Cell Biol. 2000;151(3):495–506.

26. Chen D, Xu W, Bales E, Colmenares C, Conacci-Sorrell M, Ishii S, Stavnezer E, Campisi J, Fisher DE, Ben-Ze'ev A, Medrano EE. SKI activates Wnt/beta-catenin signaling in human melanoma. Cancer Res. 2003;63(20):6626–34.

27. Pareek CS, Sachajko M, Jaskowski JM, Herudzinska M, Skowronski M, Domagalski K, Szczepanek J, Czarnik U, Sobiech P, Wysocka D, Pierzchala M, Polawska E, Stepanow K, Ogłuszka M, Juszczuk-Kubiak E, Feng Y, Kumar D. Comparative analysis of the liver transcriptome among cattle breeds using RNA-seq. Vet Sci. 2019;6(2):36.

28. Song C, Huang Y, Yang Z, Ma Y, Chaogetu B, Zhuoma Z, Chen H. RNA-seq analysis identifies differentially expressed genes insubcutaneous adipose tissuein Qaidamford cattle, Cattle-Yak, and Angus cattle. Anim (Basel). 2019;9(12):1077.

29. Liang H, Xu L, Zhao X, Pan K, Yi Z, Bai J, Qi X, Xin J, Li M, Ouyang K, Song X, Liu C, Qu M. RNA-seq analysis reveals the potential molecular mechanisms of daidzein on adipogenesis in subcutaneous adipose tissue of finishing Xianan beef cattle. J Anim Physiol Anim Nutr (Berl). 2020;104(1):1–11.

30. Ahn B, Choi MK, Yum J, Cho IC, Kim JH, Park C. Analysis of allele-specific expression using RNA-seq of the Korean native pig and Landrace reciprocal cross. Asian-Australas J Anim Sci. 2019;32(12):1816–25.

31. Li SY, Huang PH, Tarng DC, Lin TP, Yang WC, Chang YH, Yang AH, Lin CC, Yang MH, Chen JW, Schmid-Schönbein GW, Chien S, Chu PH, Lin SJ. Four-and-a-half LIM domains protein 2 is a coactivator of wnt signaling in diabetic kidney disease. J Am Soc Nephrol. 2015;26(12):3072–84.

32. Kong Y, Shelton JM, Rothermel B, Li X, Richardson JA, Bassel-Duby R, Williams RS. Cardiac-specific LIM protein FHL2 modifies the hypertrophic response to beta-adrenergic stimulation. Circulation. 2001;103(22):2731–8.

33. Rosen ED, MacDougald OA. Adipocyte differentiation from the inside out. Nat Rev Mol Cell Biol. 2006;7(12):885–96.

34. Furuhashi M, Tuncman G, Görgün CZ, Makowski L, Atsumi G, Vaillancourt E, Kono K, Babaev VR, Fazio S, Linton MF, Sulsky R, Robl JA, Parker RA, Hotamisligil GS. Treatment of diabetes and atherosclerosis by inhibiting fatty-acid-binding protein aP2. Nature. 2007;447(7147):959–65.

35. Satoh A, Stein L, Imai S. The role of mammalian sirtuins in the regulation of metabolism, aging, and longevity. Handb Exp Pharmacol. 2011;206:125–62.

36. Jeon TI, Osborne TF. SREBPs: metabolic integrators in physiology and metabolism. Trends Endocrinol Metab. 2012;23(2):65–72.

37. Wang Y, Kim KA, Kim JH, Sul HS. Pref-1, a preadipocyte secreted factor that inhibits adipogenesis. J Nutr. 2006;136(12):2953–6.

38. Amann T, Egle Y, Bosserhoff AK, Hellerbrand C. FHL2 suppresses growth and differentiation of the colon cancer cell line HT-29. Oncol Rep. 2010;23(6):1669–74.

39. Kim SY, Völkl S, Ludwig S, Schneider H, Wixler V, Park J. Deficiency of Fhl2 leads to delayed neuronal cell migration and premature astrocyte differentiation. J Cell Sci. 2019;132(6):jcs228940.

40. Chen YH, Wu ZQ, Zhao YL, Si YL, Guo MZ, Han WD. FHL2 inhibits the Id3-promoted proliferation and invasive growth of human MCF-7 breast cancer cells. Chin Med J (Engl). 2012;125(13):2329–33.

41. Wu M, Wang J, Tang W, Zhan X, Li Y, Peng Y, Huang X, Bai Y, Zhao J, Li A, Chen C, Chen Y, Peng H, Ren Y, Li G, Liu S, Wang J. FOXK1 interaction with FHL2 promotes proliferation, invasion and metastasis in colorectal cancer. Oncogenesis. 2016;5(11):e271. Published 2016 Nov 28.

42. Kurakula K, Vos M, Otermin Rubio I, Marinković G, Buettner R, Heukamp LC, Stap J, de Waard V, van Tiel CM, de Vries CJ. The LIM-only protein FHL2 reduces vascular lesion formation involving inhibition of proliferation and migration of smooth muscle cells. PLoS One. 2014;9(4):e94931. Published 2014 Apr 15.

43. Asghar U, Witkiewicz AK, Turner NC, Knudsen ES. The history and future of targeting cyclin-dependent kinases in cancer therapy. Nat Rev Drug Discov. 2015;14(2):130–46.

44. Kubben FJ, Peeters-Haesevoets A, Engels LG, et al. Proliferating cell nuclear antigen (PCNA): a new marker to study human colonic cell proliferation. Gut. 1994;35(4):530–5.

45. Zschemisch NH, Liedtke C, Dierssen U, Nevzorova YA, Wüstefeld T, Borlak J, Manns MP, Trautwein C. Expression of a cyclin E1 isoform in mice is correlated with the quiescent cell cycle status of hepatocytes in vivo. Hepatology. 2006;44(1):164–73.

46. Qie S, Diehl JA. Cyclin D1, cancer progression, and opportunities in cancer treatment. J Mol Med (Berl). 2016;94(12):1313–26.

47. Ng CF, Ng PK, Lui VW, Li J, Chan JY, Fung KP, Ng YK, Lai PB, Tsui SK. FHL2 exhibits anti-proliferative and anti-apoptotic activities in liver cancer cells. Cancer Lett. 2011;304(2):97–106.

48. Qian Z, Mao L, Fernald AA, Yu H, Luo R, Jiang Y, Anastasi J, Valk PJ, Delwel R, Le Beau MM. Enhanced expression of FHL2 leads to abnormal myelopoiesis in vivo. Leukemia. 2009;23(9):1650–7.

49. Kong L, Zhang C. LncRNA DLX6-AS1 aggravates the development of ovarian cancer via modulating FHL2 by sponging miR-195-5p. Cancer Cell Int. 2020;20:370. Published 2020 Aug 5.

50. Danen-Van Oorschot AA, van der Eb AJ, Noteborn MH. BCL-2 stimulates apoptin-induced apoptosis. Adv Exp Med Biol. 1999;457:245–9.

51. Zhao G, Zhu Y, Eno CO, Liu Y, Deleeuw L, Burlison JA, Chaires JB, Trent JO, Li C. Activation of the proapoptotic Bcl-2 protein Bax by a small molecule induces tumor cell apoptosis. Mol Cell Biol. 2014;34(7):1198–207.

52. He C, Wang Y, Xu Q, Xiong Y, Zhu J, Lin Y. Overexpression of Krueppel like factor 3 promotes subcutaneous adipocytes differentiation in goat Capra hircus. Anim Sci J. 2021;92(1):e13514.

53. Xu Q, Lin Y, Wang Y, Bai W, Zhu J. Knockdown of KLF9 promotes the differentiation of both intramuscular and subcutaneous preadipocytes in goat. Biosci Biotechnol Biochem. 2020;84(8):1594–602.

Publisher's note